

Clinical presentations and molecular studies of invasive renal epithelioid angiomyolipoma

Cheng-Keng Chuang¹  · Hsin Chia Angela Lin¹ · Han-Yu Tasi¹ · Kun-Han Lee¹ · Yuting Kao¹ · Fukai Leo Chuang¹ · Ying-Hsu Chang¹ · Po-Hung Lin¹ · Chung-Yi Liu¹ · See-Tong Pang¹

Received: 28 January 2017 / Accepted: 19 May 2017 / Published online: 25 May 2017
© Springer Science+Business Media Dordrecht 2017

Abstract

Purpose Epithelioid angiomyolipoma (EAML) is a rare variant of renal angiomyolipoma with malignant potential, and the cytogenetic and clinical behavior of EAML remains a challenging issue.

Methods We retrospectively analyze the clinical courses of five EAML, the use of everolimus on metastatic EAML, and next-generation sequencing (NGS) and polymerase chain reaction (PCR) studies to investigate the gene mutation of TSC and the impact of PI3K/Akt/mTOR signaling pathway in metastatic EAML.

Results The mean age was 37.8 years, mean tumor size was 13 cm, all patients received radical nephrectomy, one stage IV patient received neoadjuvant mTOR inhibitor management, and one patient with high mitotic activity developed metastasis 1 year after nephrectomy. NGS assay showed a frameshift gene mutation of TSC2 in chromosome 16. PCR array for the mRNA alterations in PI3K/Akt/mTOR signaling pathway of EAML showed high expression of PIP3, AKT, TSC1, mTOR, PDK1, P70, 4E-BP1 and eIF4E.

Conclusion EAML of the kidney is a specific type of renal AML with malignant potentials, where around 22% of the patients present with invasion or metastasis. Higher mitotic activities indicate a greater metastatic potential, with radical nephrectomy as the treatment of choice, and mTOR inhibitors such as everolimus either as neoadjuvant or adjuvant targeted therapy can lead to a better clinical outcome. NGS to explore the mTOR signaling pathway may help us to better understand the pathogenesis and progression of EAML.

Keywords Angiomyolipoma · Kidney · Next-generation sequencing · Mammalian target of rapamycin · Metastasis

Introduction

Renal angiomyolipoma (AML) is a benign mesenchymal tumor composed of abnormal thick-walled blood vessels, smooth muscle cells and adipose tissue [1, 2]. Most renal AMLs are sporadic, but some are associated with tuberous sclerosis complex (TSC). TSC is an autosomal dominant disorder that leads to the activation of mammalian target of rapamycin (mTOR), characterized by the development of multiple benign tumors throughout the body, with around half of the TSC patients eventually developing variable sizes of renal AMLs [3, 4]. The epithelioid angiomyolipoma of the kidney (EAML) is a rare variant of AML with malignant potential, with one-third of reported EAML cases developing metastasis [5–7]. Sensitivity to chemotherapy reagents remains controversial for invasive or metastatic EAML [8, 9]. Everolimus is one of the mTOR inhibitors. Apart from being used for cancer target therapy, it is also used in the treatment of TSC-related renal AML [10, 11] and some cases with EAML. The role of TSC on renal AML development is well established, demonstrating a loss of heterozygosity (LOH) of the TSC complex [12, 13]; however, the cytogenetic and metastatic features of EAML have not been extensively studied. Given the potentially poor prognosis associated with invasive EAML, the clinical and molecular studies of this rare entity is essential.

Materials and methods

With the approval from the Institutional Research Board (IRB), we retrospectively reviewed invasive EAML cases

✉ Cheng-Keng Chuang
ckchuang@gmail.com

¹ Chang Gung Memorial Hospital Linkou Branch, Chang Gung University, Taoyuan, Taiwan, Republic of China

in our institution. Here we present the clinical courses of these cases, the use of everolimus on metastatic EAML, and next-generation sequencing (NGS) and polymerase chain reaction (PCR) studies to investigate the gene mutation of TSC and the impact of PI3K/Akt/mTOR signaling pathway in metastatic EAML.

DNA extraction and next-generation sequencing (NGS) analysis

Genomic DNA is extracted from tumor tissues by QIAmp DNA Mini kit (QIAGEN Science, Germantown, MD, USA) according to manufacturer's instructions. The concentration and purity of DNA were measured using ND-1000 spectrophotometer (OD₂₆₀/OD₂₈₀ ratio between 1.8 and 2.0) as well as checked by electrophoresis on 1% agarose gel. Subsequently, 1.0 µg DNA per sample was used as input material for the DNA sample preparations. Sequencing libraries were generated using Truseq Nano DNA HT Sample Preparation Kit (Illumina, San Diego, CA, USA) according to manufacturer's instructions, and index codes were added to attribute sequences to each sample. The genomic DNA is randomly fragmented to a size of 350 bp by Covaris cracker, and then DNA fragments were end-polished, A-tailed and ligated with the full-length adapter for Illumina sequencing with further PCR amplification. PCR products were purified using Agencourt AMPure XP system (Beckman Coulter Life Sciences, Indianapolis, IN, USA), and libraries were analyzed for size distribution by Agilent 2100 Bioanalyzer (Agilent Technologies, Santa Clara, CA, USA) and quantified using real-time PCR. Finally, the sequencing strategy is Illumina HiSeq 4000 (150 bp, paired-end) was applied to generate 1 Gb for each sample.

PI3K-AKT signaling pathway PCR array

Changes in PI3K-AKT-related genes expression were detected by using Human PI3K-AKT Signaling Pathway RT² Profiler™ PCR Array (PAHS-058ZF-12; Qiagen). Firstly, total RNA from tumor tissues was extracted using the guanidinium-phenol-chloroform extraction method. Total RNA was reverse-transcribed into cDNA using RT2 First Strand Kit (Qiagen), followed by conducting qPCR using the RT2SYBR Green qPCR Master Mix (Qiagen) according to manufacturer's instructions. The PCR was performed with Roche LightCycler 480 apparatus (Roche Applied Science, Mannheim, Germany). Finally, gene expression was analyzed by using the Web-based RT2 Profiler PCR Array Data Analysis version 3.5 software.

Case EAML-1

A 35-year-old man suffered from dry cough for weeks and a low-grade fever for 1 day. He visited our emergency department in September 2014. There was no hematuria or flank pain. Physical examination revealed a chronically ill male with a palpable left upper quadrant mass and grade 3 left varicocele. Chest and abdominal computed tomography (CT) showed multiple lung masses, a huge mediastinal mass and a 17-cm hypervascular left renal tumor (Fig. 1a, c). Laboratory tests showed that his hemoglobin was 14.9 g/dL, serum creatinine 0.73 (eGFR 122 mL/min/1.73 m²), albumin 4.7 g/dL, LDH 219 U/L, AST 25 U/L, ALT 22 U/L, ALK-P 79 U/L and calcium 9.4 mg/dL. Under the suspicion of renal tumor with mediastinum and lung metastasis, CT-guided kidney biopsy was performed which disclosed solid sheets of epithelioid tumor cells with abundant eosinophilic granular or vesicular cytoplasm, moderate pleomorphic nuclei and focal necrosis. Immunohistochemical (IHC) staining was positive for vimentin, HMB-45, Melan-A and cytokeratin (AE1/AE3); partially positive for actin, CD10; and negative for CK7, PAX-8, RCC, S-100 protein and desmin. The diagnosis of metastatic EAML was thus confirmed. The patient was then started on 10 mg everolimus daily since October 2014 with grade 1–2 mucositis and fatigue. Follow-up CT scans in January 2015 showed a decrease in size of the renal tumor (from 17 to 12 cm) and mediastinal mass (from 6.6 to 3.4 cm) and a regressive change with a decrease in size and number of bilateral lung lesions (Fig. 1b, d). A cytoreductive left nephrectomy was performed in March 2015, where the tumor mitotic count was 1–2 per 10 high-power field (HPF). Postoperative course was uneventful, and the patient restarted everolimus 1 month after nephrectomy with the dose reduced to 5 mg daily because of grade 2–3 nausea, vomiting, anorexia, fatigue, malaise and muscle aching. Follow-up chest CT showed a further decrease in size of the lung nodules. To investigate the kind of sequence variants on a genomic scale in the tumor tissue, NGS assay of the tumor region and nonmalignant kidney tissue from this patient was performed. PCR array for the mRNA alterations in PI3K/Akt/mTOR signaling pathway was determined.

Case EAML-2

A 58-year-old male presented to our hospital with chronic cough and body weight loss of more than 15 kg over the past 6 months. Imaging studies including abdominal CT and bone scans revealed a 13-cm right kidney tumor with IVC tumor thrombus, with a tentative staging of T3bN0M0. Right nephrectomy and thrombectomy with cardiopulmonary bypass were performed in April 2015. The IHC staining of the tumor was positive for HMB-45, Melan-A and vimentin, and the mitotic count was 6 per 10

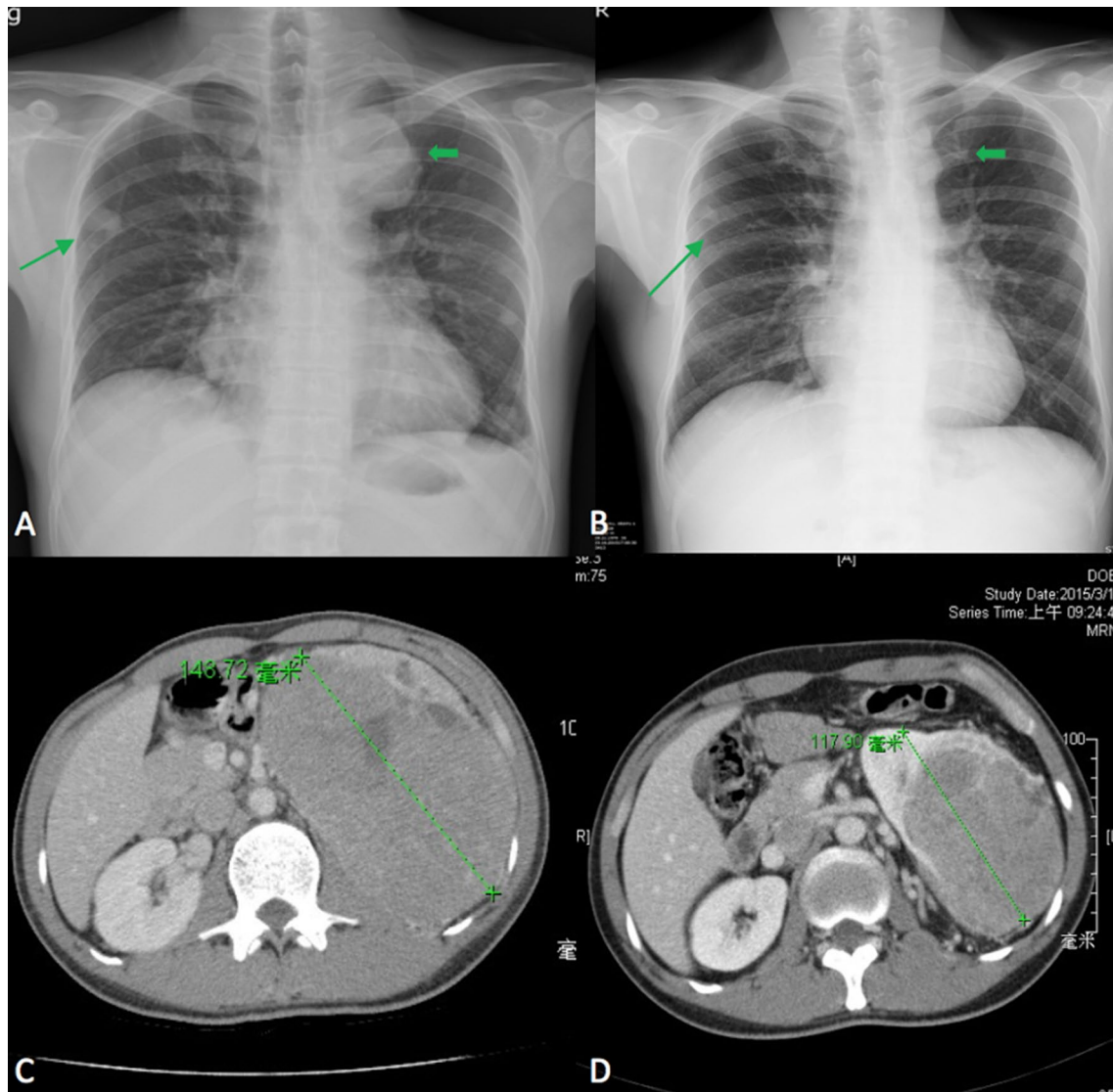


Fig. 1 Imaging studies of EAML-1 patient show multiple lung nodules, mediastinal mass and left renal tumor (a, c), after 6 months of everolimus treatment the lung lesions almost disappear, and there is a decrease in size of mediastinal mass and renal tumor (b, d)

HPF. Postoperative follow-up with CT scans showed free of recurrence until March 2016 where local recurrence and IVC tumor thrombosis appeared, and multiple metastases involving the liver and bone. Ten milligram everolimus daily was prescribed since then. Six months later, in October 2016, CT showed a regression of the IVC thrombus, from 18.4 to 15.9 cm, but left renal vein encasement was found.

Case EAML-3

An 18-year-old female presented with a sudden onset of diffuse abdominal pain in February 2005 where a 17-cm left renal tumor with IVC invasion was found. Left radical nephrectomy with IVC thrombectomy and

cardiopulmonary bypass was performed, and postoperative recovery was uneventful. IHC staining was positive for HMB-45, smooth muscle actin and vimentin. Mitotic activity was rare. She has been regularly followed up at our hospital since then, with no recurrence till now, 12 years after surgery.

Case EAML-4

A 38-year-old female suffered from painless hematuria in July 2014 and was found to have a 4.8-cm tumor in her right kidney, where right renal vein and IVC tumor thrombi were noted. She underwent right nephrectomy and thrombectomy without cardiopulmonary bypass. IHC staining was positive for HMB-45, smooth muscle

actin and vimentin, and the mitotic activity was 0–1 per 10 HPF. The patient was disease-free at the time of writing this paper.

Case EAML-5

A 40-year-old male suffered from hematuria and flank pain for 2 weeks, there was 5 kg body weight loss in 3 months, and CT image found a 12-cm left renal tumor. He received left radical nephrectomy in February 2016 that disclosed a 12.3-cm tumor with over 70% of atypical epithelioid area and left renal vein tumor thrombus (pT3aN0). The mitotic activity was 2 per 10 HPF, and necrosis area was 50% of the tumor specimen. IHC staining was positive for HMB-45, Melan-A, smooth muscle actin, and negative for AE1/AE3. Follow-up abdominal CT in October 2017 was free of recurrence.

Results

Clinical characteristics

From the chart and image reviews of 23 EAML cases in our institution, five patients (22%) presented as locally advanced or metastatic. As shown in Table 1, the mean age of these five patients was 37.8 years; the presenting symptoms include hematuria, body weight loss, cough

and abdominal pain. Four-fifth of the EAML tumor was huge, with the size ranging from 12 to 17 cm. One patient was stage IV when diagnosed. All patients received radical nephrectomy, one received neoadjuvant mTOR inhibitor management, and two IVC thrombectomies were performed with cardiopulmonary bypass. One patient (EAML-2) with high mitotic activity (6 per 10 HPF in the EAML tumor and 3 per 10 HPF in the IVC tumor thrombus) had recurrence and developed multiple metastases 1 year after nephrectomy. Another patient (EAML-3) whose tumor mitotic activity was very rare had been followed up over 12 years without any evidence of recurrence.

Molecular studies

The NGS assay result for EAML-1 is shown in Table 2, where 33 genes were identified in the chromosomes, including 28 genes with single-point mutation. It is noteworthy that gene mutation of TSC2 was observed in chromosome 16 that had been represented with frameshift deletion. Meanwhile, nonsynonymous SNV at IRS2 formed stop codon, let translation of amino acid early stopped and caused dysfunction. Subsequently, we also demonstrated that deletion mutation certainly occurred in TSC2, but not in IRS by Sanger sequencing. It may be speculated that frequency of IRS mutation was too low to be detected by Sanger sequence, but only measured by NGS analysis. As shown in Fig. 2, the result of gene sequencing analysis

Table 1 Invasive EAML patient characteristics

Case	EAML-1	EAML-2	EAML-3	EAML-4	EAML-5
Age/gender	35/M	58/M	18/F	38/F	40/M
Location	Left	Right	Left	Right	Left
Symptoms	Dry cough and fever	Cough and BW loss	Abdominal pain	Hematuria	Hematuria, flank pain and BW loss
Tumor size	17 cm	13 cm	17 cm	4.8 cm	12.3 cm
Stage at presentation	IV (lung and mediastinum)	III (T3b)	III (T3b)	III (T3b)	III (T3a)
IVC thrombus	N	Y	Y	Y	N
Nephrectomy	Y	Y	Y	Y	Y
IVC thrombectomy		Y	Y	Y	
Cardiopulmonary bypass		Y	Y		
Follow-up status	Live with disease	Local recurrence and metastases to bone and liver	Disease-free	Disease-free	Disease-free
Follow-up time	28 months	22 months	143 months	30 months	11 months
Everolimus	Neoadjuvant and adjuvant	After metastasis			
Survival	y	y	y	y	y
Mitotic activity(/HPF)	1–2/10	5–6/10	Rarely found	0–1/10	2/10
HMB-45 staining	Positive	Positive	Positive	Positive	Positive

M male; *F* female; *N* no involvement; *Y* yes; *IVC* inferior vena cava; *HPF* high-power field; *BW* body weight

Table 2 List of sequence variants identified by NGS on the EAML-1

Gene name	Chromosome al locus	Nucleotide change	Protein change	Reference sequence	Exons	Mutation type
PRAMEF4	1p36.21	c.G503A	p.C168Y	NM 001009611	exon3	missense SNV
DUSP27	1q24.1	c.G3001C	p.V1001L	NM 001080426	exon5	missense SNV
CDC73	1q31.2	c.C720T	p.S240S	NM 024529	exon7	synonymous SNV
METAP1D	2q31.1	c.C449A	p.S150Y	NM 199227	exon4	missense SNV
UGT1A7	2q37.1	c.T622C	p.W208R	NM 019077	exon1	missense SNV
TACC3	4p16.3	c.G664A	p.E222 K	NM 006342	exon4	missense SNV
P4HA2	5q31.1	c.T968G	p.L323R	NM 001017973	exon8	missense SNV
PCDHB4	5q31.3	c.C1422A	p.A474A	NM 018938	exon1	synonymous SNV
RAMP3	7p13	c.G228T	p.E76D	NM 005856	exon3	missense SNV
MUC12	7q22.1	c.C4995T	p.S1665S	NM 001164462	exon2	synonymous SNV
MUC17	7q22.1	c.C1629T	p.T543T	NM 001040105	exon3	synonymous SNV
PPAPDC1B	8p11.23	c.T485G	p.F162C	NM 001102559	exon6	missense SNV
MSR1	8p22	c.C1158T	p.V386 V	NM 138715	exon9	synonymous SNV
ZFAND1	8q21.13	c.A189G	p.P63P	NM 001170796	exon4	synonymous SNV
KNDC1	10q26.3	c.G2092A	p.E698 K	NM 152643	exon14	missense SNV
OR56B4	11p15.4	c.T389C	p.I130T	NM 001005181	exon1	missense SNV
KCNJ11	11p15.1	c.G96C	p.R32S	NM 000525	exon1	missense SNV
ANO2	12p13.31	c.G563A	p.R188Q	NM 001278596	exon4	missense SNV
NCOR2	12q24.31	c.A1491G	p.Q497Q	NM 001077261	exon16	synonymous SNV
IRS2	13q34	c.G594A	p.W198X	NM 003749	exon1	stopgain
CBLN3	14q12					
GOLGA6L10	15q25.2	c.T471A	p.S157S	NM 001164465	exon6	synonymous SNV
TP53TG3D	16p11.2	c.T324C	p.G108G	NM 001243722	exon1	synonymous SNV
TSC2	16p13.3	c.2153delG	p.R718 fs	NM 000548	exon20	frameshift deletion
TBC1D3 K	17q12	c.T364A	p.L122 M	NM 001001418	exon6	missense SNV
MUM1	19p13.3	c.T763C	p.S255P	NM 032853	exon5	missense SNV
ZNF442	19p13.2	c.A844T	p.R282X	NM 030824	exon6	stopgain
ZNF428	19q13.31					
FAM83D	20q11.23	c.C461A	p.A154D	NM 030919	exon1	missense SNV
TTPAL	20q13.12	c.C916T	p.P306S	NM 001039199	exon5	missense SNV
	21p11.2					
HS6ST2	Xq26.2	c.G609T	p.R203S	NM 001077188	exon3	missense SNV
ESX1	Xq22.2	c.G822A	p.A274A	NM 153448	exon4	synonymous SNV
TREX2	Xq28	c.C615T	p.A205A	NM 080701	exon2	synonymous SNV

The NGS sequencing has also highlighted IRS2 and TSC2 mutation, and the downstream gene is PI3K/Akt/mTOR signaling pathway. It is noteworthy that gene mutation of TSC2 was observed in chromosome 16 that had been represented with frameshift deletion

revealed that tumor sample certainly existed with deletion of G and nucleotide C left-shift compared with that of the paired normal sample (at arrow site) (Fig. 2). PCR array for the mRNA alterations in PI3K/Akt/mTOR signaling pathway of EAML indicated that the mRNA levels of PI3K, AKT, TSC1, mTOR, PDK1, P70, 4E-BP1 and eIF4E were >twofold in tumor tissue compared to the paired normal tissue in the same patient (Table 3). Among them, 4E-BP1 was 20.6-fold high expression. Our IHC staining result revealed that the level of mTOR phosphorylation in EAML-1–EAML-5 cases had higher than this in

AML-1–AML-5 (Fig. 5). Using Western blot, the protein expressions of PI3K/Akt/mTOR signaling pathway-related factors, including TSC1, TSC2, p70 and S6 kinase in renal tissues of EAML-1 and two cases of renal AML, are illustrated in Fig. 4. The renal TSC1 and TSC2 expressions were reduced, but S6K and total phosphorylated forms of p70 were increased in the tumor region of EAML-1 compared with normal sample from the same case. This suggests that mTOR inhibitors may provide therapeutic benefit in the treatment of invasive or metastatic EAML by upregulation of 4E-BP1 expression.

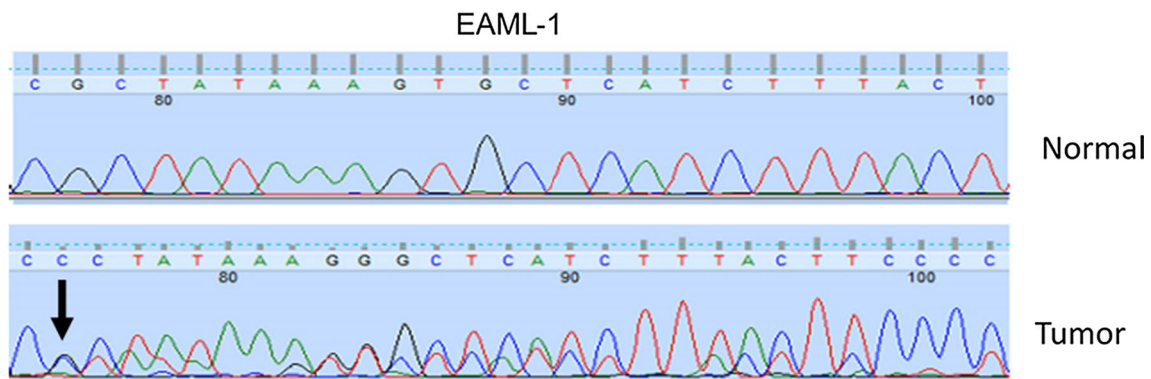


Fig. 2 Detection of *TSC2* gene mutation in epithelioid angiomyolipoma EAML-1. The sequence chromatograms of the *TSC2* gene derived from EAML-1 tumor sample and paired normal sample are shown. Mutation sites are indicated by arrows in the exon region

Table 3 PCR array for the mRNA alterations in PI3K/Akt/mTOR signaling pathway

Gene symbol	Fold regulation
PDK1	34.65
PIK3CA	2.7
PIK3CG	6
PIK3R1	4.04
PIK3R2	3.82
AKT1	2.63
TSC1	2.94
mTOR	2.3
4E-BP1	20.6
eIF4E	2.02
p70	2.47

Discussion

Renal AML is a common benign neoplasm characterized by abnormal thick-walled blood vessels, smooth muscles and adipose tissue. Most renal AMLs are sporadic and asymptomatic if the tumor size is small. As the tumor grows, it can cause serious problems such as bleeding because of its abnormal vasculature and can lead to the need for immediate management such as nephrectomy, partial nephrectomy or transcatheter arterial embolization (TAE) [14, 15]. Tuberous sclerosis complex (TSC) is an autosomal dominant disorder characterized by multiple benign tumors throughout the body, including the brain, skin, lungs and kidneys. Renal manifestations in TSC cause significant burdens. In contrast to classical AMLs, epithelioid AML (EAML), one of the AML variants, has a distinct common morphology and immunohistochemical features [16]. In 2004, the World Health Organization (WHO) classification of renal neoplasms defines EAML as a potentially malignant mesenchymal neoplasm,

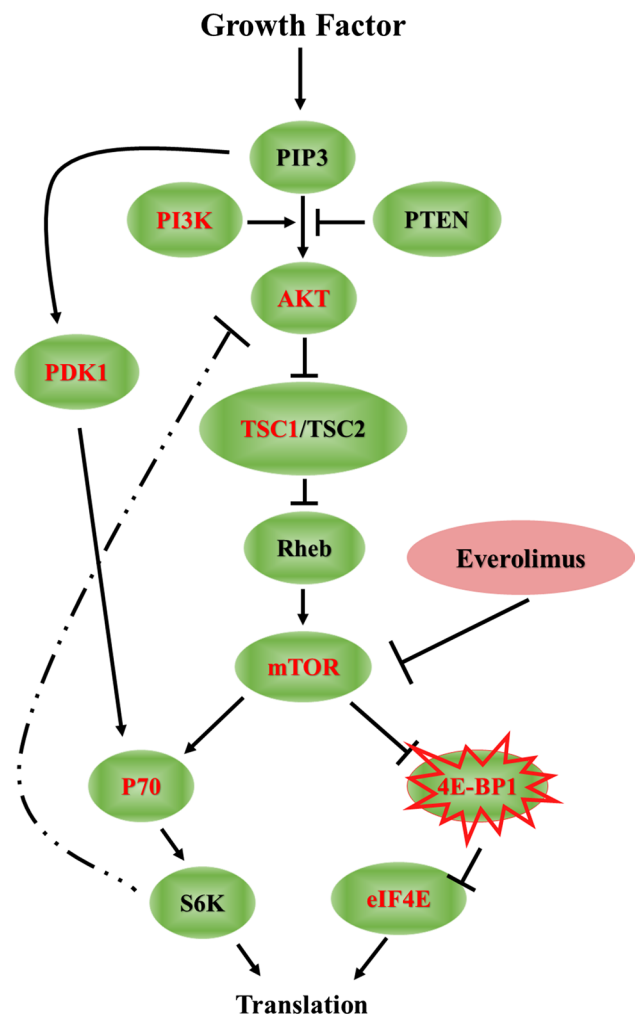


Fig. 3 Schematic representation of PI3K/Akt/mTOR signaling pathway. The expression patterns of PI3K/Akt/mTOR signaling pathway molecules in EAML-1 were determined by PI3K-AKT signaling PCR array. The mRNA expression in tumor tissue with more than twofold overexpression as compared to the paired normal tissue is labeled in red [31]. The 4E-BP1 was 20.6-fold high expression

characterized by the proliferation of predominantly epithelioid cells with metastatic potentials. EAML behaves much more aggressively and is capable of malignant transformation, recurrence, metastasis and fatal outcome. Most EAMLs might be initially misdiagnosed as renal cell carcinoma (RCC) or sarcoma, especially if they morphologically appear without the adipose component [17]. Radical nephrectomy remains the standard of care for this aggressive disease, and the cytotoxic chemotherapy response remains controversial [8, 9]. Not all the EAML develops metastasis, large tumor size, tumor necrosis, and the presence of venous invasion, and high mitotic activity (>2 mitotic figures/10 HPF) was highly associated with malignant behavior [18, 19]. In our observation, the tumors with rare mitotic activity (EAML-3 and EAML-4) were disease-free after radical nephrectomy even though they initially presented with locally advanced status, but the patient with high mitotic activity (3–6 mitotic activity/10 HPF) in tumor tissue developed multiple metastases 1 year after nephrectomy. Aggressive treatment for high-risk EAML should consider adjuvant therapy including either chemotherapy or mTOR inhibitor. For metastatic EAML, mTOR inhibitors or multikinase inhibitors were reported to have their clinical efficacy [20, 21].

In the target therapy era, there are still lacks of sufficient evidence to support neoadjuvant treatments for large unresectable renal tumors, with high-level vascular invasion and venous thrombus [22]. Neoadjuvant therapy may sometimes be used to downsize and downstage large and/or unresectable tumors [23], not only in hepatic tumor but also may change radical nephrectomy to nephron-sparing surgery [24].

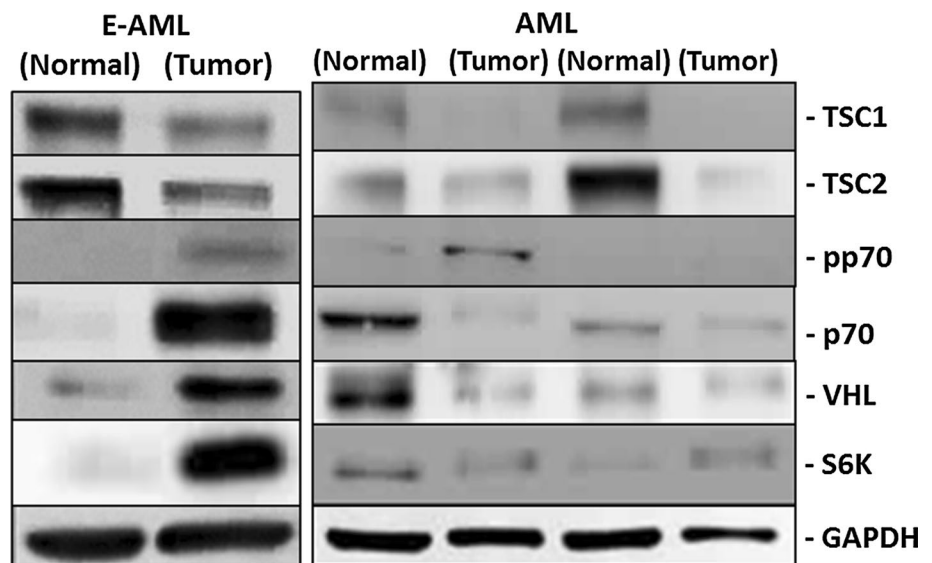
Genetic analysis showed that the three types of AMLs, including the AML, EAML and TSC-related renal AML,

shared the same allelic loss on chromosome arm 16p [6, 25–27]. However, evidence for the relationship between the AML, EAML and the malignant transformation is still lacking. The *TSC1* and *TSC2* genes encode for harmartin and tuberlin, respectively, and are tumor suppressor genes. Both are involved in the Rheb/mTOR/p70S6 kinase signaling pathway. Mutation in these genes result in an mTORC1(mammalian target of rapamycin complex-1)-dependent activation of the hypoxia-inducible factor (HIF) and upregulate the expression of vascular endothelial factor, which will increase the angiogenesis and tumor growth [28, 29]. Our current results from the mRNA (Fig. 3) and protein (Fig. 4) expression of PI3K/Akt/mTOR signaling cascades in renal tissue of an EAML case found that there is frameshift mutation of *TSC2* and downregulation of TSC1/TSC2 protein level, subsequently inducing increased levels of mTOR. Therefore, treating this case with everolimus clinically may reasonably lead to two phenomena in tumor tissues. One, the upregulation of 4E-BP1 suppresses the translational process and results in reduced tumor cell proliferation, and the other is presented with the increase of total and phosphorylated form of p70 protein in our study (Fig. 5).

Based on these findings, we speculated that the mechanism on the decrease of tumor size, cell proliferation and translational process was due to the increase of 4E-BP1 expression in the renal tumor of the EAML patient after mTOR inhibitor treatment.

The functional relationship between TSC1/TSC2 and mTORC1 has led to the use of mTOR inhibitors in several clinical manifestations of TSC, including TSC-associated renal AMLs [30]. Everolimus is an oral, active analogue of rapamycin, which acts as a signal transduction inhibitor, and targets the activity of mTOR. Its efficacy has been

Fig. 4 Western blot analysis of PI3K/Akt/mTOR signaling pathway in EAML and AML tumor and paired normal samples. The renal TSC1 and TSC2 expressions were reduced, but S6K and total phosphorylated forms of p70 were increased in the tumor region of EAML-1 compared with normal sample from the same case



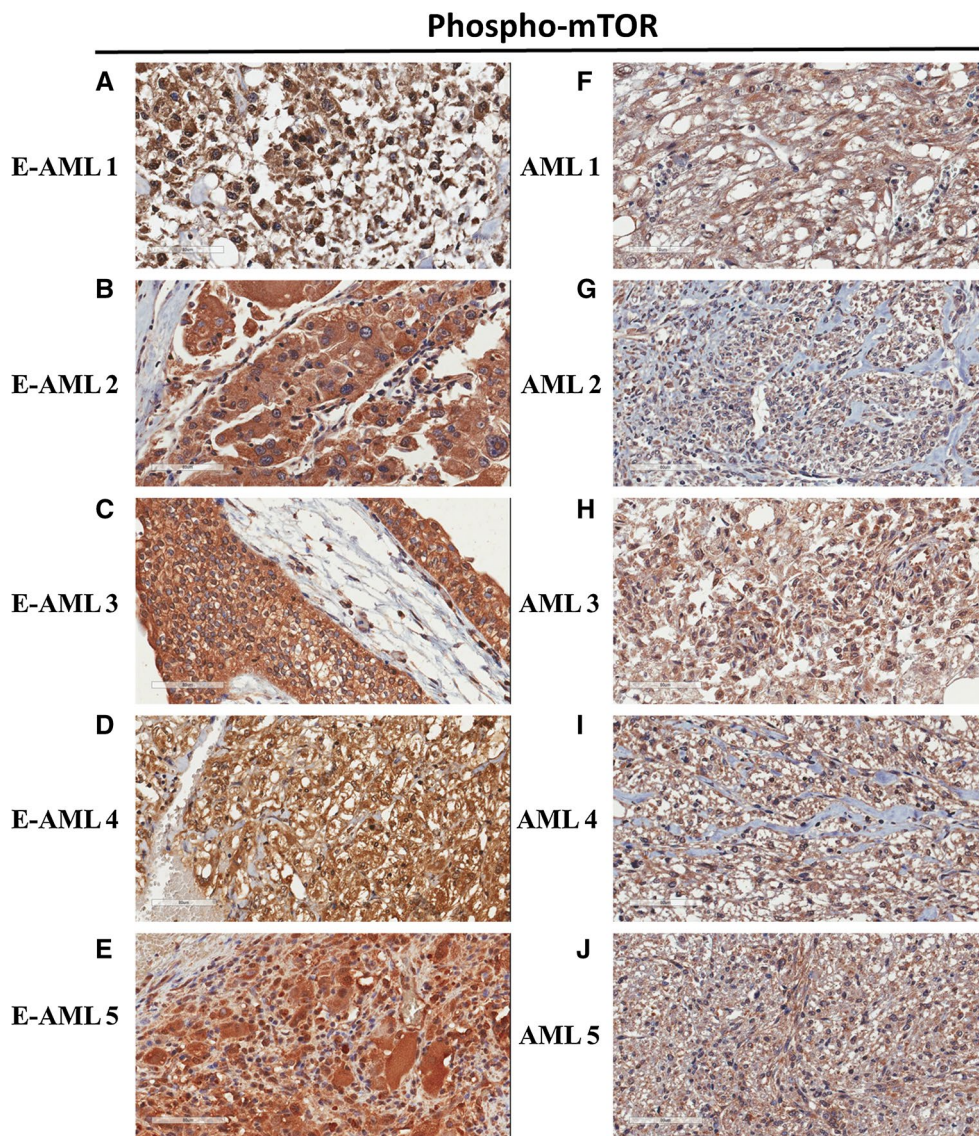


Fig. 5 Representative IHC staining of phospho-mTOR on EAML (a–e) and AML (f–j). Images are presented as 200× magnification

established in TSC-related AMLs, neuroendocrine tumors and renal cell carcinomas [9, 10]. Finding out whether there is a common signaling pathway in the development of these different types of AMLs or each of them having their own *TSC* genetic mutation, or whether the mTOR pathway participates in advanced/metastatic EAML, as well as the *TSC* gene status, may help us explore the pathogenesis of EAML, malignant transformation and their management. The *TSC* gene status should also be considered in EAML.

Conclusions

Epithelioid angiomyolipoma (EAML) of the kidney is a specific type of renal AML with malignant potentials,

where around 22% of the patients present with invasion or metastasis. The most common metastatic sites are lungs, liver and lymph nodes. For a young patient with a huge renal mass and less fat content, the diagnosis of EAML should be considered, and renal biopsy along with positive IHC staining for HMB-45 can confirm the diagnosis. Higher mitotic activities in EAML tumor specimen indicate a greater metastatic potential, with radical nephrectomy as the treatment of choice, and mTOR inhibitors such as everolimus either as neoadjuvant or as adjuvant targeted therapy can lead to a better clinical outcome. It would also be valuable to perform next-generation sequencing on more EAML samples and explore the mTOR signaling pathway in more detail in order for us to better understand the pathogenesis and progression of EAML.

Acknowledgements We thank the National Science Council of the Republic of China, Chang Gung Molecular Medicine Research Center and Chang Gung Memorial Hospital for financial aid: NSC 105-2314-B-182-024-MY3, CMRPG1A0051-2, CMRPG3A0811-3.

Funding This study was funded by National Science Council of Taiwan (NSC 105-2314-B-182-024-MY3) and Chang Gung Memorial Hospital (CMRPG1A0051-2, CMRPG3A0811-3).

Compliance with ethical standards

Conflict of interest We declare that we have no conflict of interest.

Ethical approval This study was approved by IRB of Chang Gung Medical Foundation (IRB 104-7555C). All procedures performed in studies involving human participants were in accordance with the ethical standards of the institutional and/or national research committee and with the 1964 Declaration of Helsinki and its later amendments or comparable ethical standards.

References

- Amin MB (2004) Epithelioid angiomyolipoma. In: Eble JN, Sauter G, Epstein JI, Sesterhenn IA (eds) WHO classification of tumours. Pathology and genetics. Tumors of the urinary system and male genital organs. IARC Press, Lyon, pp 68–69
- Eble JN, Sauter G, Epstein JI, Sesterhenn IA (2004) Pathology and genetics of tumours of the urinary system and male genital organs. Lyon IARC 90:109
- Van Slegtenhorst M, De Hoogt R, Hermans C, Nellist M, Jansen B, Verhoef S, Lindhout D, Van den Ouweland A, Halley D, Young J (1997) Identification of the tuberous sclerosis gene TSC1 on chromosome 9q34. *Science* 277(5327):805–808
- Consortium ECTS (1993) Identification and characterization of the tuberous sclerosis gene on chromosome 16. *Cell* 75(7):1305–1315
- Brimo F, Robinson B, Guo C, Zhou M, Latour M, Epstein JI (2010) Renal epithelioid angiomyolipoma with atypia: a series of 40 cases with emphasis on clinicopathologic prognostic indicators of malignancy. *Am J Surg Pathol* 34(5):715–722
- Martignoni G, Pea M, Bonetti F, Zamboni G, Carbonara C, Longa L, Zancanaro C, Maran M, Brisigotti M, Mariuzzi G (1998) Carcinoma-like monotypic epithelioid angiomyolipoma in patients without evidence of tuberous sclerosis: a clinicopathologic and genetic study. *Am J Surg Pathol* 22(6):663–672
- Huang K-H, Huang C-Y, Chung S-D, Pu Y-S, Shun C-T, Chen J (2007) Malignant epithelioid angiomyolipoma of the kidney. *J Formos Med Assoc* 106(2):S51–S54
- Yamamoto T, Ito K, Suzuki K, Yamanaka H, Ebihara K, Sasaki A (2002) Rapidly progressive malignant epithelioid angiomyolipoma of the kidney. *J Urol* 168(1):190–191
- Cibas ES, Goss GA, Kulke MH, Demetri GD, Fletcher CD (2001) Malignant epithelioid angiomyolipoma (sarcoma ex angiomyolipoma) of the kidney: a case report and review of the literature. *Am J Surg Pathol* 25(1):121–126
- Bissler JJ, Kingswood JC, Radzikowska E, Zonnenberg BA, Frost M, Belousova E, Sauter M, Nonomura N, Brakemeier S, de Vries PJ (2016) Everolimus for renal angiomyolipoma in patients with tuberous sclerosis complex or sporadic lymphangiomyomatosis: extension of a randomized controlled trial. *Nephrol Dial Transp* 31(1):111–119
- Sampson JR (2009) Therapeutic targeting of mTOR in tuberous sclerosis. Portland Press Limited, London
- Sepp T, Yates J, Green AJ (1996) Loss of heterozygosity in tuberous sclerosis hamartomas. *J Med Genet* 33(11):962–964
- Pan C-C, Jong Y-J, Chai C-Y, Huang S-H, Chen Y-J (2006) Comparative genomic hybridization study of perivascular epithelioid cell tumor: molecular genetic evidence of perivascular epithelioid cell tumor as a distinctive neoplasm. *Hum Pathol* 37(5):606–612
- Chang Y-H, Wang L-J, Chuang C-K, Wong Y-C, Wu C-T, Hsieh M-L (2007) The efficacy and outcomes of urgent superselective transcatheter arterial embolization of patients with ruptured renal angiomyolipomas. *J Trauma Acute Care Surg* 62(6):1487–1490
- Yip K, Peh W, Tam P (1998) Spontaneous rupture of renal tumours: the role of imaging in diagnosis and management. *Br J Radiol* 71(842):146–154
- Delgado R, Bojorge BdL, Albores-Saavedra J (1998) Atypical angiomyolipoma of the kidney. *Cancer* 83(8):1581–1592
- Švec A, Velenská Z (2005) Renal epithelioid angiomyolipoma—a close mimic of renal cell carcinoma. Report of a case and review of the literature. *Pathol Res Pract* 200(11):851–856
- He W, Cheville JC, Sadow PM, Gopalan A, Fine SW, Al-Ahmadie HA, Chen Y-B, Oliva E, Russo P, Reuter VE (2013) Epithelioid angiomyolipoma of the kidney: pathological features and clinical outcome in a series of consecutively resected tumors. *Mod Pathol* 26(10):1355–1364
- Nese N, Martignoni G, Fletcher CD, Gupta R, Pan C-C, Kim H, Ro JY, Hwang IS, Sato K, Bonetti F (2011) Pure epithelioid PEComas (so-called epithelioid angiomyolipoma) of the kidney: a clinicopathologic study of 41 cases: detailed assessment of morphology and risk stratification. *Am J Surg Pathol* 35(2):161–176
- Shitara K, Yatabe Y, Mizota A, Sano T, Nimura Y, Muro K (2011) Dramatic tumor response to everolimus for malignant epithelioid angiomyolipoma. *Jpn J Clin Oncol* 41(6):814–816
- Lee D-W, Chang H, Kim Y-J, Kim K-M, Lee H-J, Lee J-S (2014) Sorafenib-induced tumor response in a patient with metastatic epithelioid angiomyolipoma. *J Clin Oncol* 32(11):e42–e45
- Schrader AJ, Steffens S, Schnoeller TJ, Schrader M, Kuczyk MA (2012) Neoadjuvant therapy of renal cell carcinoma: a novel treatment option in the era of targeted therapy? *Int J Urol* 19(10):903–907
- Bergamo F, Maruzzo M, Basso U, Montesco MC, Zagonel V, Gringeri E, Cillo U (2014) Neoadjuvant sirolimus for a large hepatic perivascular epithelioid cell tumor (PEComa). *World J Surg Oncol* 12(1):46
- Borregales LD, Adibi M, Thomas AZ, Wood CG, Karam JA (2016) The role of neoadjuvant therapy in the management of locally advanced renal cell carcinoma. *Ther Adv Urol* 8(2):130–141
- Martignoni G, Pea M, Rigaud G, Manfrin E, Colato C, Zamboni G, Scarpa A, Tardanico R, Roncalli M, Bonetti F (2000) Renal angiomyolipoma with epithelioid sarcomatous transformation and metastases: demonstration of the same genetic defects in the primary and metastatic lesions. *Am J Surg Pathol* 24(6):889–894
- Carbonara C, Longa L, Grosso E, Mazzucco G, Borrone C, Garrè ML, Brisigotti M, Filippi G, Scabar A, Giannotti A (1996) Apparent preferential loss of heterozygosity at TSC2 over TSC1 chromosomal region in tuberous sclerosis hamartomas. *Genes Chromosom Cancer* 15(1):18–25
- Henske EP, Neumann HP, Scheithauer BW, Herbst EW, Short MP, Kwiatkowski DJ (1995) Loss of heterozygosity in the tuberous sclerosis (TSC2) region of chromosome band 16p13 occurs in sporadic as well as TSC-associated renal angiomyolipomas. *Genes Chromosom Cancer* 13(4):295–298

28. Karbowniczek M, Henske EP (2005) The role of tuberlin in cellular differentiation: Are B-Raf and MAPK involved? *Ann N Y Acad Sci* 1059(1):168–173
29. Brugarolas JB, Vazquez F, Reddy A, Sellers WR, Kaelin WG (2003) TSC2 regulates VEGF through mTOR-dependent and-independent pathways. *Cancer Cell* 4(2):147–158
30. El-Hashemite N, Zhang H, Henske EP, Kwiatkowski DJ (2003) Mutation in TSC2 and activation of mammalian target of rapamycin signalling pathway in renal angiomyolipoma. *Lancet* 361(9366):1348–1349
31. Lam JS, Pantuck AJ, Belldegrun AS, Figlin RA (2007) Protein expression profiles in renal cell carcinoma: staging, prognosis, and patient selection for clinical trials. *Clin Cancer Res* 13(2):703s–708s. doi:[10.1158/1078-0432.Ccr-06-1864](https://doi.org/10.1158/1078-0432.Ccr-06-1864)